

Chapter 2

Mechanism of Dry Etching

A guiding principle for designing a dry etching process has yet to be established. However, guidelines for designing a process may be obtained by examining the reaction processes. For that, one must first understand the mechanism of dry etching. This chapter starts with the basics of plasma and goes on to describe the dry etching reaction processes and the mechanism of anisotropic etching without relying on mathematical equations or difficult theories, in a way that is completely accessible to readers who have no background in dry etching.

In the discussion on the fundamentals of plasma, all the topics for understanding dry etching mechanisms are covered, including “What is a plasma?”, the plasma parameters, and the collisions and reactions that take place in the plasma.

Then there is a discussion on the behaviors of ions, which play an important role in realizing an anisotropic etching. Specific numerical values associated with the ion sheath thickness and mean free path are provided to help readers deepen their understanding of the ion scattering phenomena in the ion sheath. Next, a discussion on the dry etching reaction processes, mechanisms of anisotropic etching, and parameters that determine the etch rates and selectivity provides guidelines on how to select gases, set pressures, and build the process.

2.1 Basics of Plasma

2.1.1 What Is a Plasma?

This section begins with a simple description of plasma. Plasma refers to an “ionized gas,” in which approximately the same numbers of electrons and ions exist; it is in an electrically neutral state from a macroscopic viewpoint. The electron density (n_e) and ion density (n_i) are substantially equal to one another, and they are referred to as the plasma density. Because electrons are able to travel freely

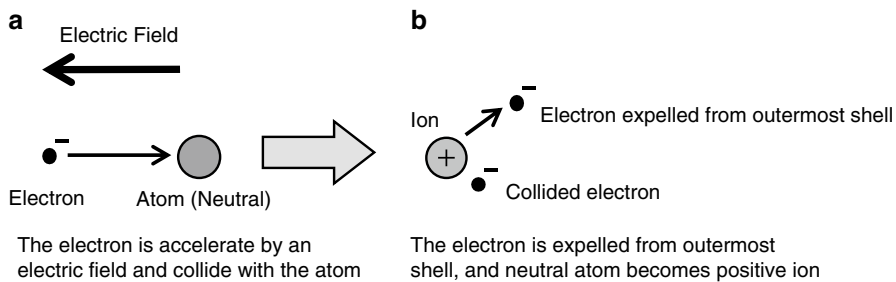
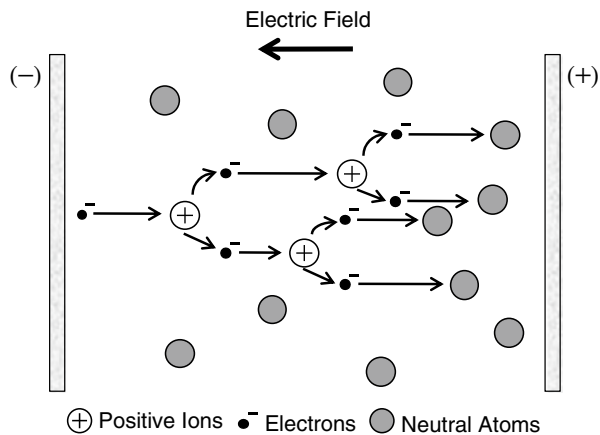


Fig. 2.1 Ion generation by the collision of electrons and neutral atoms

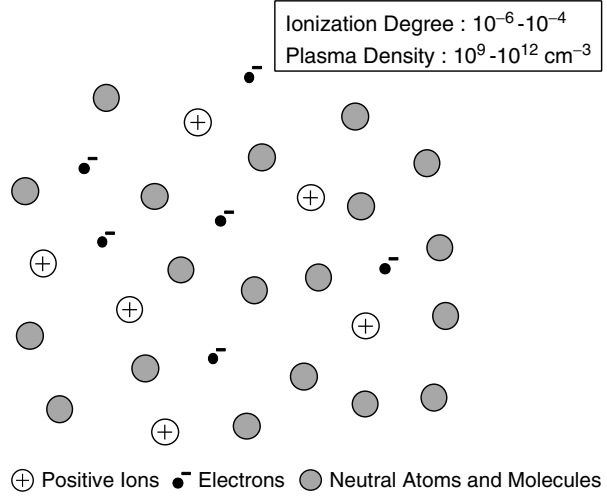
Fig. 2.2 Principle of gas discharge



within the plasma, it has a conductive property. When a radiofrequency (RF) power is applied on a pair of electrodes in an etch chamber, electrons are accelerated by an electric field generated by the RF power, acquire kinetic energy, and collide with atoms and molecules (Fig. 2.1a). If the kinetic energy of an electron is greater than the ionization energy (ionization voltage), the electron in the outermost shell of the atom or molecule is expelled. As a result, the neutral atom or the molecule turns into an ion (Fig. 2.1b). On the other hand, the electron that has been expelled from the molecule or the atom adds to the first colliding electron to now make a total of two electrons. These electrons are then accelerated under the electric field, collide with other atoms and molecules, and generate new ions and electrons. The number of ions and electrons increase as in an avalanche and eventually exceed a threshold level over which a resulting discharge begins and creates a plasma. This mechanism is summarized in Fig. 2.2.

The plasma is classified into a completely ionized plasma, in which 100% of electrons and ions are ionized, and a weakly ionized plasma, in which the degree of ionization is low and a mixture of ions, electrons, and neutral atoms and molecules coexist. A glow discharge is used for dry etching. A plasma generated by the glow

Fig. 2.3 Schematic of glow discharge plasma (weakly ionized plasma)



discharge is categorized as a weakly ionized plasma and consists of equal numbers of positive and negative charges, as well as electrically neutral atoms and molecules. Figure 2.3 shows a model diagram for a glow discharge plasma. The degree of ionization in a glow discharge plasma is on the order of 10^{-6} – 10^{-4} . In other words, the degree of ionization is around 1 out of every 10,000 at most. The majority of the particles remain neutral, and only one ion and one electron exist for every 10,000 neutral particles. This is why it is called a weakly ionized plasma. The number of gas molecules at a pressure of 13.3 Pa (100 mTorr) is around $3.5 \times 10^{15} \text{ cm}^{-3}$, so the plasma density at a ionization degree of 10^{-4} is $3.5 \times 10^{11} \text{ cm}^{-3}$. The plasma density of a glow discharge plasma is within a range of 10^{-9} – 10^{-12} cm^{-3} .

2.1.2 Plasma Parameters

Table 2.1 shows typical values for the plasma parameters associated with an arc discharge plasma, which is a strongly ionized plasma, and a glow discharge plasma, which is a weakly ionized plasma [1, 2]. A glow discharge plasma is characterized by a lack of thermal equilibrium between the electron temperature T_e and gas temperature T_g . An electron temperature corresponds to the energy of the electrons, and its relationship to the kinetic energy $\frac{1}{2}m_e v_e^2$ is expressed as

$$\frac{1}{2}m_e v_e^2 = \frac{3}{2}kT_e \quad (2.1)$$

where m_e is the electron mass, v_e is the electron velocity, and k is Boltzmann's constant.

Table 2.1 Types of plasma and plasma parameters [1, 2]

Type of plasma		Plasma density (cm ⁻³)	Electron temperature T_e (K)	Ion temperature T_i (K)	Gas temperature T_g (K)
Arc discharge	Strongly ionized plasma (high-temperature plasma)	$>10^{14}$	6,000	6,000	6,000
Glow discharge	Weakly ionized plasma (low-temperature plasma)	$10^9\text{--}10^{12}$	$\sim 10^4$	300–1,000	300

Because electrons are very light, they are accelerated by the electrical field and acquire a large kinetic energy. The average electron energy in a glow discharge plasma is several electron-volts. Say the electron energy is 2 eV; then the electron temperature T_e is 23,200 K, according to Eq. (2.1). On the other hand, the temperature of the neutral atoms and molecules, which is the gas temperature T_g , is around room temperature (293 K). In other words, $\frac{T_e}{T_g}$ is around 80, and the electron

temperature T_e and gas temperature T_g are not in a thermal equilibrium. Although the electrons have an energy level comparable to a high temperature of 10^4 K or higher, the etch chamber and the wafer remain at low temperature because the electron mass is small. For this reason, a glow discharge plasma is also referred to as a low-temperature plasma. Because electrons have enough energy for causing the excitation, ionization, and dissociation of atoms and molecules, with the gas temperature remaining at close to the room temperature, diverse types of reactions are possible at low temperature. This is the reason why the glow discharge plasma is used for semiconductor manufacturing.

An arc discharge is a strongly ionized plasma, and its plasma density is 10^{14} cm⁻³ or greater. The electron temperature T_e , ion temperature T_i , and gas temperature T_g are in a thermal equilibrium, and $T_e = T_i = T_g$ is approximately 6,000 K. For this reason, the arc discharge is referred to as a high-temperature plasma.

2.1.3 Collision Processes in a Plasma

Electrons that have gained energy in a plasma collide with atoms and molecules. These collisions are categorized as elastic collisions and inelastic collisions. Figure 2.4 summarizes the collision processes in a plasma. With an elastic collision, only the kinetic energy changes; the internal energy does not change. This type of collision tends to take place when the electron energy is low. In the example in Fig. 2.4, the electron is bounced back in a different direction. Because a portion of the electron's energy is transferred into the kinetic energy of the atom, the atom slightly gains a velocity. The electron loses a small amount of energy

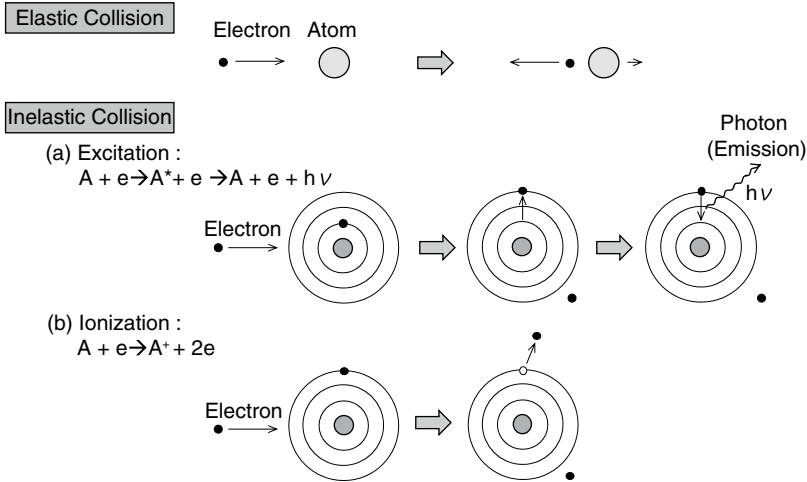
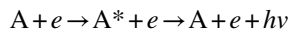


Fig. 2.4 Collision processes in a plasma

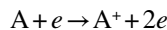
through the collision. With an inelastic collision, the internal energies are converted, and excitation, ionization, dissociation, and electron attachment take place, described next.

1. **Excitation:** A colliding electron provides energy to the bound electron in an atom and enables it to jump to a higher energy level. In general, the excited state is unstable, and the excited electron would be able to remain in this state for only around 10^{-8} s, and then returns to the ground state. Photon is emitted during this transition. The plasma glows because of this principle. An excitation reaction step is described as follows:

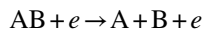


where A represents a neutral atom, and A^* represents A in an excited state. h is Planck's constant, and ν is the frequency of the emitted light.

2. **Ionization:** As mentioned earlier, an electron in the outermost shell is expelled when the energy of the colliding electron is larger than the ionization voltage, and the neutral atom turns into a positive ion. This reaction step is described as follows:

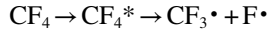


3. **Dissociation:** Dissociation occurs when the energy given by the colliding electron is larger than the binding energy of the molecule. This reaction step is described as follows:

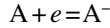


When a molecule is dissociated, its byproducts are chemically more active than the original molecule and turn into highly reactive particles. A particle in

this activated state is called a radical. It has been reported that CF_4 would easily be dissociated into a CF_3 radical ($\text{CF}_3 \cdot$) and F radical ($\text{F} \cdot$) once excited [3]. This reaction step is described as follows:



4. Electron attachment: The colliding electron attaches to the atom and turns it into a negative ion. This reaction step is described as follows:



2.2 Ion Sheath and Ion Motion in the Sheath

2.2.1 Ion Sheath and V_{dc}

V_{dc} is an extremely important parameter for understanding the dry etching mechanism and is thus described first here. In the parallel-plate dry etching equipment [reactive-ion etching (RIE)] shown in Fig. 2.5, a lower electrode, on which a wafer is placed, is connected to an RF power supply through a blocking capacitor, and the opposite electrode (upper electrode) is connected to the ground. A frequently used RF frequency is 13.56 MHz; in other words, the direction of the electric field changes 13.56×10^6 times every second. Because electrons have a small mass, they are able to follow the oscillation of the electric field. On the other hand, ions are much heavier, with masses that are approximately 100,000 times larger, and they are unable to follow the RF oscillation and do not move much from where they are. As a result, only the electrons accelerated by the electric field jump into the electrodes. Because the lower electrode is connected to a blocking capacitor, it is gradually biased to a negative potential. A direct current (DC) bias that is thus generated is referred to as a self-bias and is represented by V_{dc} . While the V_{dc} value is dependent on the RF power, it would be in the tens of volts to several hundreds of volts for

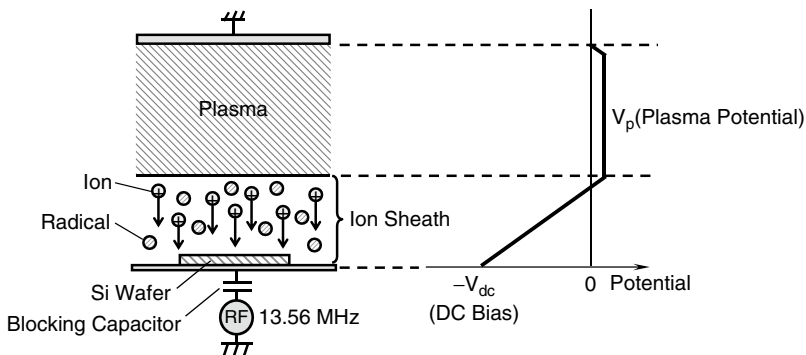
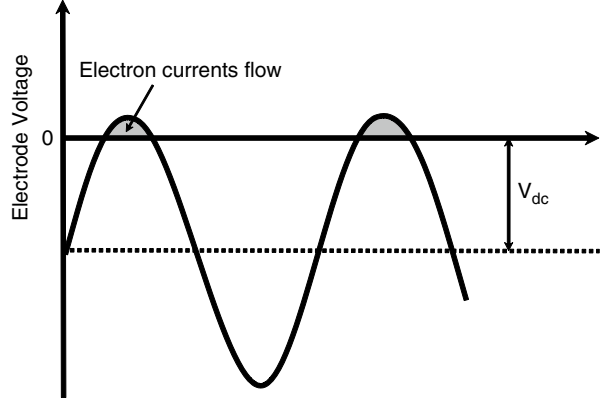


Fig. 2.5 Ion sheath and V_{dc}

Fig. 2.6 Voltage waveform at the lower electrode in an RF discharge



the etching of conductive materials such as Si and Al. Figure 2.6 shows the voltage waveform at the lower electrode in a steady state. The electrode voltage turns positive only for a small period of time during each cycle. Electron currents flow onto the electrode during this period. On the other hand, ion currents flow almost continuously. The sum of the amounts of injected charges in each cycle is zero in a steady state.

Electrons are pushed away when the electrode is negatively biased, and almost no electrons exist near the electrode. This region is called the ion sheath, with the analogy being the sheath of a sword. In other words, an ion sheath refers to a sheath filled with ions. Because the electron density is very low in this region, the probability of collision excitation is low, and almost no light is emitted. For this reason, an ion sheath is also referred to as a dark space.

Figure 2.5 shows an electrical potential distribution inside the etch chamber. As mentioned earlier, the plasma is electrically conductive, and the plasma is at equipotential from a macroscopic viewpoint; for this reason, ions travel in random directions in the plasma. The electrical potential of the plasma is referred to as the plasma potential V_p . On the other hand, ions approaching the interface between the plasma and the ion sheath are accelerated toward the wafer due to the $-V_{dc}$, which creates a potential gradient inside the ion sheath and toward the lower electrode. Here, the ions acquire the energy equivalent to $V_p + V_{dc}$. Etching is driven mainly by these ions, which travel in a straight direction, and an anisotropic profile, with small dimensional shifts from the mask patterns, is obtained. This mechanism is described in detail in the next section.

The magnitude of voltage induced at the electrodes is dependent on the ratio of the electrode surface areas. Say that the surface areas of electrodes 1 and 2 are S_1 and S_2 , respectively, and the voltages induced at each electrode are V_1 and V_2 , respectively, as shown in Fig. 2.7. Their relationship [4] would be

$$\frac{V_1}{V_2} = \left(\frac{S_2}{S_1} \right)^4 \quad (2.2)$$

Fig. 2.7 Relationship between the electrode area ratio and the voltages induced at electrodes

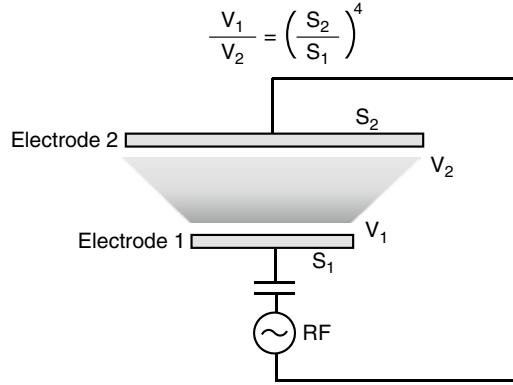
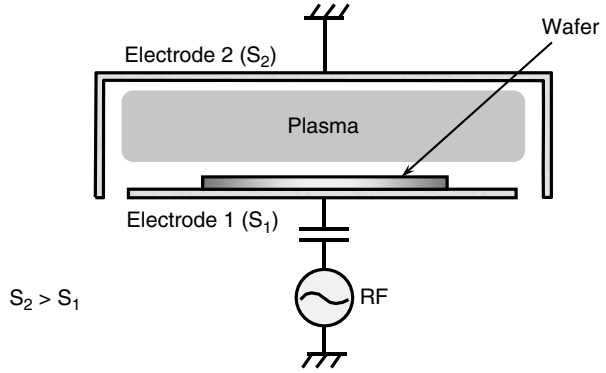


Fig. 2.8 Electrode area ratio in RIE system



In other words, a higher voltage is induced at the electrode with a smaller surface area. In general, the electrode (electrode 2) that opposes the electrode (electrode 1) on which the wafer is placed has a much larger surface area in the RIE system, so that an adequate V_{dc} is achieved at the wafer. As shown in Fig. 2.8, the chamber walls are normally held at the same electrical potential as electrode 2 in the RIE system, so that the structure helps make S_2 larger than S_1 . Because the V_{dc} induced at the chamber walls is small in this instance, sputtering on the walls is suppressed, and as a result there is an added advantage of suppressing the release of impurities, such as heavy metals from the chamber walls.

2.2.2 Ion Scattering in the Sheath

Let's now quantitatively examine the scattering of ions in the sheath. The ion sheath thickness (d_{is}) is represented by the following Child–Langmuir equation [5]:

$$d_{is} = \frac{2}{3} \left(\frac{\epsilon_0}{i_{io}} \right)^{\frac{1}{2}} \left(\frac{2e}{m_i} \right)^{\frac{1}{4}} (V_p - V_{dc})^{\frac{3}{4}} \quad (2.3)$$

Table 2.2 Calculated sheath thickness and related constants of high-density plasma [6]

<i>Conditions</i>	
Gas	Ar
Gas pressure	1.33 Pa
Mean free path (λ)	5 mm
$V_{dc}-V_p$	-100 V
Ion current density	15 mA/cm ²
<i>Calculated results</i>	
Ion sheath thickness (d_{is})	0.28 mm

where i_{io} is the ion current density, ϵ_0 is the permittivity of vacuum, e is the elementary electric charge, m_i is the ion mass, and V_p is the plasma potential.

Table 2.2 shows an example of the ion sheath thickness calculated for a high-density plasma [6]. The ion sheath thickness would pretty much be at this value for high-density plasmas such as the inductively coupled plasma (ICP) and the electron-cyclotron resonance (ECR) plasma, which are described in Chap. 4. In this example, the ion sheath thickness is calculated for Ar at a pressure of 1.33 Pa (10 mTorr) and an ion current density of 15 mA/cm². The ion sheath thickness d_{is} is extremely small, at 0.28 mm.

Another important concept in examining the scattering of ions in the sheath is the mean free path (λ), which we briefly discuss here. A mean free path is an average distance that a particle travels from one collision to the next. In other words, it is the distance over which a particle is able to travel without a collision. The mean free path will be longer at a lower gas pressure because fewer molecules exist. In other words, the lower the pressure, the longer the particle will be able to travel without a collision. The mean free path is inversely proportional to pressure. In the example shown in Table 2.2, the mean free path of Ar is 5 mm at 1.33 Pa, and it becomes 50 mm when the pressure is reduced to 0.133 Pa.

The scattering of ions in an ion sheath is examined by comparing the ion sheath thickness with the mean free path. In other words, when the mean free path is adequately larger than the ion sheath thickness, ions go through almost no scattering upon their arrival at the wafer. This directionality of ions is an important factor for enabling the anisotropic etching to be discussed in the next section.

We'll now compare the scattering of ions in an ion sheath with high-density plasma etching (e.g., ICP and ECR) and with the batch RIE (Fig. 2.9). The ion current density in a high-density plasma etcher is one order of magnitude larger than in the batch RIE. This high-density plasma etcher offers high etch rates and at the same time has a smaller ion sheath thickness. With a high-density plasma such as ICP and ECR, the sheath thickness d_{is} is thin at 0.28 mm. On the other hand, the mean free path λ is long at 5 mm because of the lower operating pressure of 1.33 Pa.

In other words, λ is much larger compared to d_{is} ($\frac{d_{is}}{\lambda} = 0.056$), and the majority of

ions arrive at the surface of the sample without colliding with neutral particles in the sheath (Fig. 2.9a). On the other hand, λ is smaller than d_{is} in the batch RIE

($\frac{d_{is}}{\lambda} = 3.8$), and most of the ions collide with neutral particles in the sheath and are scattered (Fig. 2.9b).

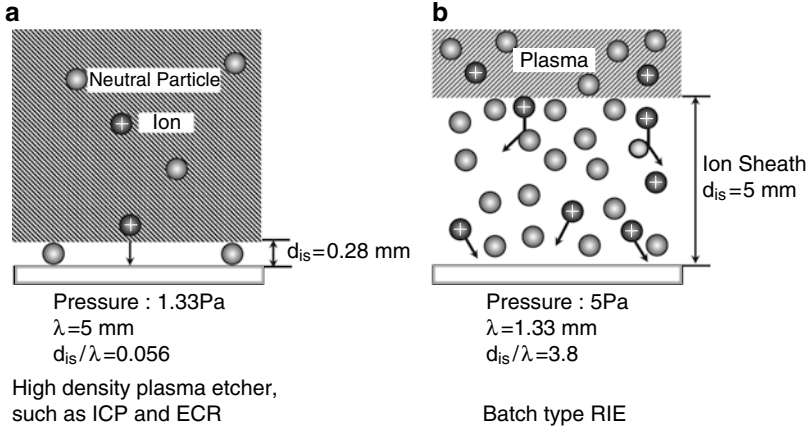
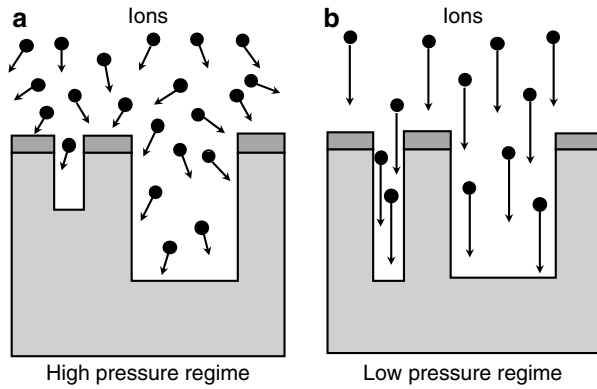


Fig. 2.9 Ion scattering in the ion sheath

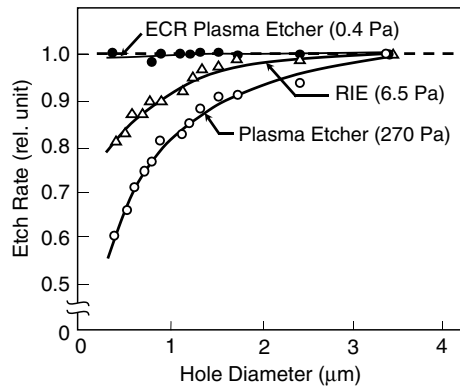
Fig. 2.10 Effect of the ion direction on fine patterning



As thus explained, ion scattering in the sheath in the high-density plasma etcher is almost nonexistent, and there are very few ions coming in at an angle.

Figure 2.10 illustrates the effect of the ions' travel direction on fine patterning. When there are a large number of ions coming in at an angle due to scattering, fewer ions are able to enter fine patterns, as Fig. 2.10a shows, and the etch rate drops. On the other hand, an adequate number of ions are able to enter patterns with large openings, and the etch rate does not suffer. In other words, the etch rate becomes pattern-dependent. This issue can be resolved by using a lower-pressure regime, which prevents ions from being scattered and coming in at angles. As Fig. 2.10b shows, ions that are traveling highly directionally are able to etch fine patterns and wider patterns at the same etch rate. Figure 2.11 illustrates this phenomenon, based on the study of the various types of etchers [6]. In plasma etcher with a high operating pressure of 270 Pa, the etch rate of contact holes strongly depends on the hole size. The etch rate drastically decreases below a diameter of 1.0 μm . The decrease

Fig. 2.11 Etch rates of contact holes as a function of hole diameter and operating pressure in three different etches [6]



in the etch rate is 40 % at a diameter of 0.4 μm . On the other hand, the ECR plasma etcher with a low operating pressure of 0.4 Pa shows a plateau in the etch rate characteristics down to a diameter of 0.4 μm , because there are enough incoming ions even in smaller holes.

2.3 How to Design Dry Etching Processes

2.3.1 Reaction Processes in Dry Etching

As mentioned at the beginning of this chapter, it is necessary first to examine the reaction processes in order to obtain the guidelines for designing a dry etching process. Let's now go over the basic concepts involved.

Dry etching proceeds in the following four steps: (1) Reactive species (neutral radicals and ions) are generated in the plasma; (2) species are transported and adsorb on the etch target film; (3) reactions take place at the surface of the etch target film, and etch byproducts are created; and (4) etch byproducts desorb from the surface of the etch target film. Figure 2.12 shows the reaction steps when Si is etched with CF_4 [7]. First, CF_4 dissociates into CF_3 radicals ($\text{CF}_3\cdot$) and F radicals ($\text{F}\cdot$) in the plasma.

Next, the CF_3 radicals adsorb on the Si surface and react with Si to form etch byproducts SiF_4 . SiF_4 desorbs from the Si surface, and the etching thus proceeds.

In order to realize fine patterning, it is important to process with a high level of fidelity to the mask patterns. Figure 2.13 illustrates the differences between the isotropic and anisotropic etching. When radicals drive the etching reaction, the etching proceeds not only in the vertical direction, but also in the horizontal direction, as Fig. 2.13a shows, because the radicals move randomly by Brownian motion. This is referred to as isotropic etching, and it results in undercut under the mask and makes fine patterning difficult. On the other hand, as Fig. 2.13b shows, an etching that proceeds in a vertical direction would enable processing that closely replicates the mask patterns. This is referred to as anisotropic etching.

- (1) Reaction species (neutral radicals and ions) are generated in the plasma
- (2) Species are transported and adsorb on the target etch film
- (3) Reaction takes place at the target etch film surface, and byproducts are created
- (4) Byproducts desorb from the target etch film surface

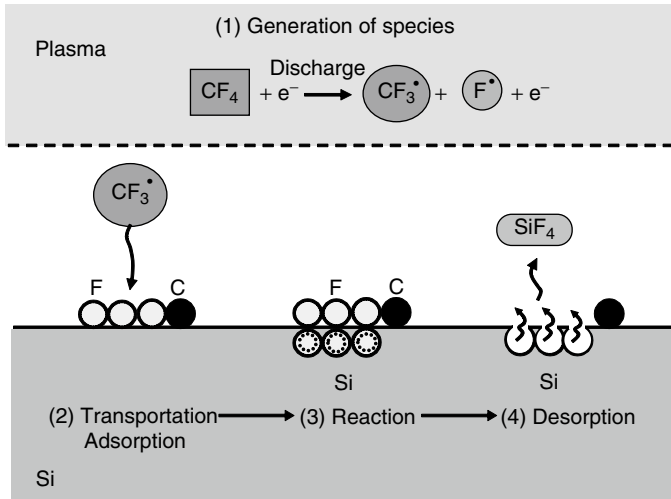


Fig. 2.12 Reaction steps of dry etching for the case of Si etching with CF_4 [7]

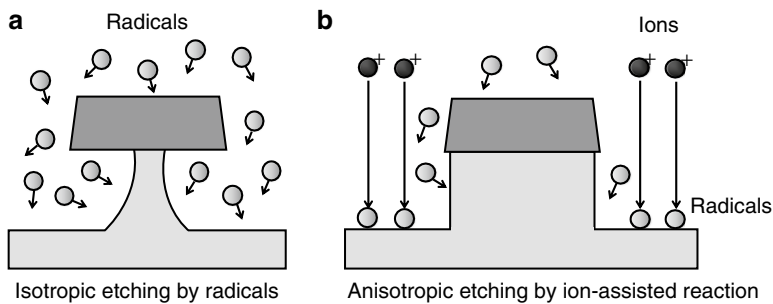


Fig. 2.13 Isotropic and anisotropic etching

2.3.2 Mechanism of Anisotropic Etching

Let's first consider how to achieve anisotropic etching. The basic approach to the implementation of anisotropic etching is to make the surface reaction proceed only in the vertical direction. Ion-assisted reactions are one approach to achieving this objective. An ion-assisted reaction is a phenomenon in which the incoming ions enhance the surface reactions. In a system in which ion-assisted reactions take

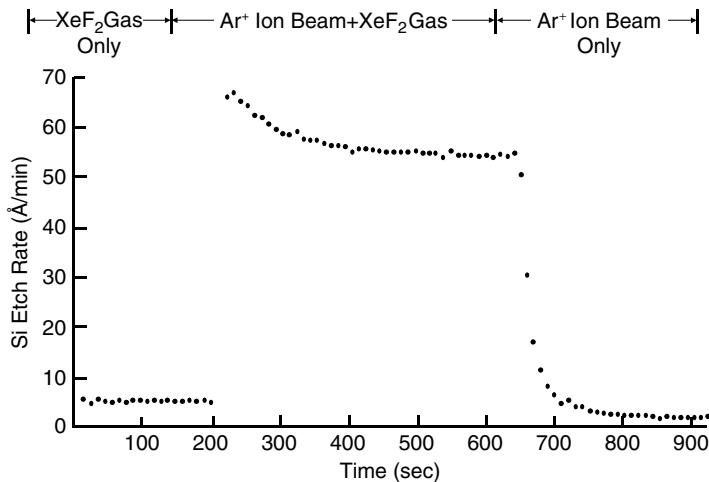


Fig. 2.14 Ion-assisted etching [8]

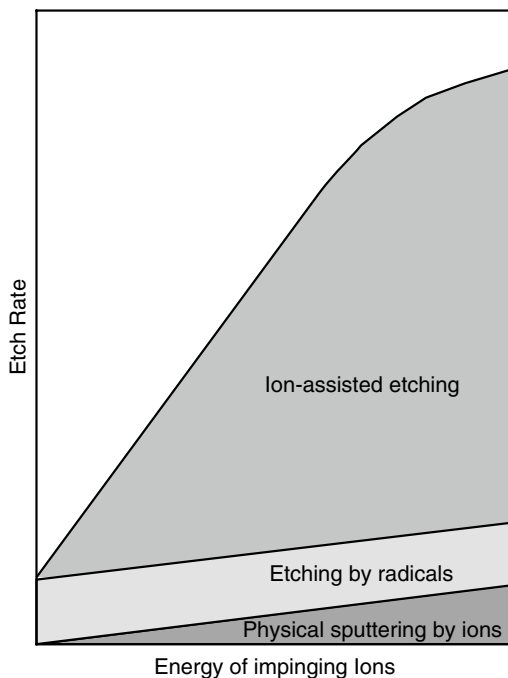
place, the etch rate of an ion-irradiated surface is significantly larger than the etch rate by neutral radicals. Therefore, an anisotropic etching is realized by making the ions strike the etch target surface at normal incidence.

Figure 2.14 shows the experimental result that explains the ion-assisted reactions [8]. The vertical axis in the figure represents the Si etch rate. First, Si is etched with only the XeF₂ gas. In this instance, Si is etched by the F radicals dissociating from XeF₂, but the etch rate is low, around 5 Å/min at most. The etch rate, on the other hand, increases by a factor of 10 or more when this reaction system is irradiated with Ar⁺ ions at 450 eV. Next, when the supply of XeF₂ is halted, and only the Ar⁺ ions are irradiated, the etch rate decreases drastically to 3 Å/min or less with only the physical sputtering by ions. This type of phenomenon is called the ion-assisted etching, in which the ion bombardment is given to the adsorbed radicals and the etch rate increases. The rate of etching would otherwise be extremely low when it is only by the radicals or by physical sputtering. There are several theories for the ion-assisted reaction. The most widely believed theory is the “hot spot model,” in which the temperature of the areas under the ion irradiation becomes very high locally, and the etch rate goes up as a result of a significant boost to the radical reactions [9].

Because the rate of etching through the ion-assisted reactions is orders of magnitude larger than the rate of etching by radicals, as thus shown, it is possible to obtain an anisotropic etch profile when ions come in on the wafer vertically, so that the etch rate in the vertical direction (by assisted reactions) is faster than the rate of etching in the horizontal direction (by radicals). This is the principle of anisotropic etching by ion-assisted reactions.

Figure 2.15 shows the etch rate for each etching component as a function of the energy of impinging ions. Physical sputtering by ions is energy-dependent, and the etch rate increases with increasing ion energy. However, the etch rate itself is low.

Fig. 2.15 Etch rate for each etching component as a function of energy of impinging ions



Chemical etching driven by radicals is not dependent on the energy, and so the rate always remains constant. The etch rate is also low. The etch rate of ion-assisted etching is extremely dependent on the ion energy, and the etch rate drastically increases with increasing ion energy. Anisotropic etching is realized through ion-assisted etching.

The effects of ion-assisted etching vary among various combinations of the etch target materials and etching gases. In other words, depending on the combinations of the etch target materials and etching gases, the ion-assisted reaction may or may not occur. Figure 2.16 shows the chemical sputtering yield of Si resulting from Cl^+ , Br^+ , and F^+ ion bombardment as a function of ion energy [10], and Fig. 2.17 shows the chemical sputtering yield of Al, B, C, and Si resulting from Cl^+ ion bombardment as a function of ion energy [9]. Here, the chemical sputtering yield is defined as a difference between the sputtering yield per ion and the physical sputtering yield [9]. According to Fig. 2.16, the chemical sputtering yield strongly depends on the ion energy when Si is etched with Cl^+ and Br^+ . In other words, an ion-assisted reaction takes place with these combinations, and anisotropic etching is possible. On the other hand, there is a small dependence on the ion energy when Si is etched with F^+ ions. That is, the effect of the ion-assisted reaction is small, and anisotropic etching is less likely to take place. In the actual process, etch gases such as Cl_2 and HBr , which dissociate and generate the Cl^+ and Br^+ ions, are suited for anisotropic etching of Si. This is the reason why these gases are used as the base gases for the

Fig. 2.16 Chemical sputtering yield of Si resulting from Cl^+ , Br^+ , and F^+ ion bombardment as a function of ion energy [10]

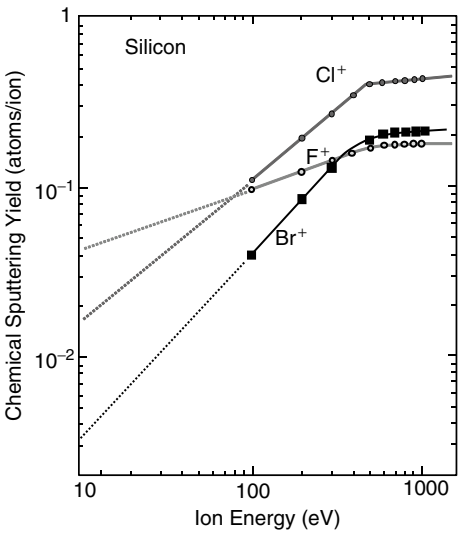
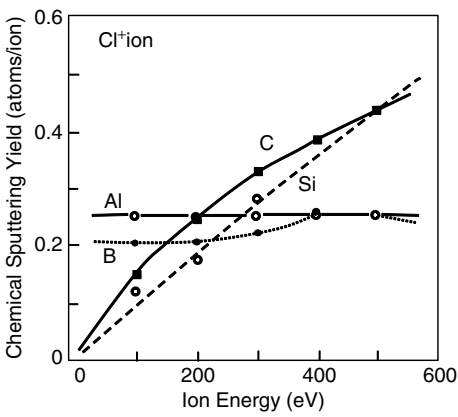


Fig. 2.17 Chemical sputtering yield of Al, B, C, and Si resulting from Cl^+ ion bombardment as a function of ion energy [9]



etching of poly-Si gates and shallow trench isolations (STIs). On the other hand, etching tends to become isotropic when Si is etched with gases like SF_6 and CF_4 , which dissociate and generate the F^+ ions.

We'll now consider Al etching. According to Fig. 2.17, the chemical sputtering yield shows no dependence on the ion energy when Al is etched with Cl^+ ions. In other words, no ion-assisted reactions take place with this combination, and etching proceeds isotropically.

In order to achieve anisotropic etching with a system in which an ion-assisted reaction does not take place at all, or in a system where the effects of ion-assisted reactions are small, as thus shown, a process with sidewall protection is used.

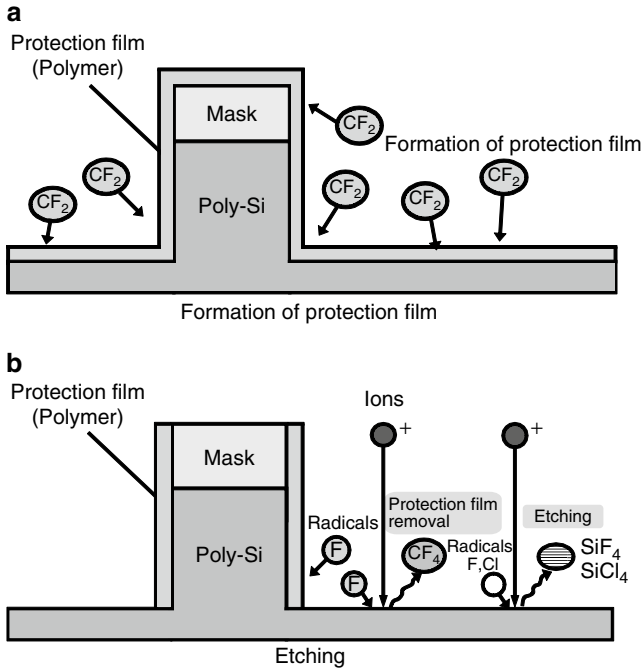


Fig. 2.18 Model for sidewall protection process [11]

2.3.3 Sidewall Protection Process

A sidewall protection process refers to a process in which the sidewalls of the etch target surface are protected with a protective film like polymer, and the protective film prevents invasion by radicals during etching. The protective film is formed when inorganic materials like SiO_2 or organic polymers are generated in the plasma. Figure 2.18 shows a model illustrating the sidewall protection process [11]. In this example, the protective film consists of organic polymers. In the case of using a mixture gas in which a gas for polymer formation is added to a main etch gas, monomers such as CF and CF_2 are generated from the additive gas. These monomers adsorb on the etch target surface and form the polymers.

As a result, the entire etch target surface is covered with polymers (Fig. 2.18a). Because ions come in vertically against the wafer, the ions remove the polymers on the horizontal surface, and the etching proceeds through the reactions between the exposed etch target material and the ions and radicals. On the other hand, because polymers are not stripped off and remain on the pattern sidewalls, where there are almost no incoming ions, the sidewalls remain protected by the polymers. Because the polymers prevent the attack of radicals on the sidewalls, an anisotropic etching is realized (Fig. 2.18b). This is the fundamental mechanism of the sidewall

protection process. The reactions in parts (a) and (b) of Fig. 2.18 have been described separately here; they take place at the same time as the actual etching.

The monomers, which are the basis of polymer formation, are sometimes generated from the main etch gas itself. Furthermore, they may also be generated when the resist is etched. When Al is etched with a Cl-based gas chemistry, the etching should be isotropic in theory, because the ion-assisted reactions do not occur. In reality, however, an anisotropic profile is obtained. The reason for this is a supply of C and H resulting from the resist being etched, which forms the sidewall protection film.

As mentioned earlier, the effect of ion-assisted reactions is very small when Si is etched using an F-based gas like SF_6 . In this case, SiO_2 would be generated when O_2 is added to the gas, and it forms a sidewall protection film. An anisotropic profile can then be obtained.

2.3.4 Etch Rate

The etch rate is related to all four of the reaction steps. In particular, surface reactions and desorption of etch byproducts are important considerations in selecting the etching gas. Some useful references are, first, the chemical sputtering yield, which was discussed earlier, and, second, the vapor pressures of etch byproducts. Figure 2.19 shows the vapor pressure curves in a simplified form. The figure shows that, in general, fluorides have higher vapor pressures than the chlorides. A higher vapor pressure means the etch byproduct is more volatile. In other words, when a gas chemistry that generates the fluorides is used, the etch byproducts desorb more

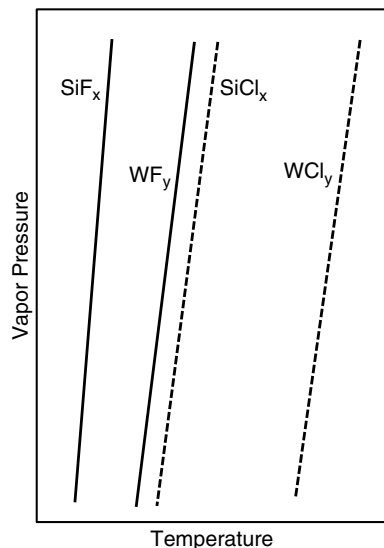


Fig. 2.19 Vapor pressure curves

Table 2.3 Melting and boiling points for various halides [12]

Halide	Melting point (°C)	Boiling point (°C)
SiF ₄	−77 (2 atm)	−95 (sublimation)
SiCl ₄	−70	57.6
SiBr ₄	5.2	153.4
WF ₆	2.5	17.5
WCl ₆	275	346.7
AlF ₃	1,290	–
AlCl ₃	190 (2.5 atm)	183 (sublimation)
AlBr ₃	97.5	255
CuF	908	1,100 (sublimation)
CuCl	452	1,367
CuBr	504	1,345

easily and the etch rate becomes higher. Data in Table 2.3 show the melting and boiling points for various halides [12]. They also show that the fluorides of Si and W tend to vaporize more easily than the chlorides. However, there is an opposite trend with Al, and the fluorides are less easy to vaporize than the chlorides. This indicates that it is possible to etch Al with a Cl-based gas, not with an F-based gas. Also, it should be noted that Al fluorides tend to result in particles, requiring caution. Table 2.4 shows the temperatures at which the various chemical compounds achieve a vapor pressure of 1,333 Pa (10 Torr) [13]. The pressure of 1,333 Pa has been chosen because it is assumed that a dry etching process would take place below this pressure. Based on this table, it is possible to figure out how easily each byproduct vaporizes and use it as a guideline for increasing the etch rates. The *Handbook of Chemistry* should be used as a reference when it is necessary to find the vapor pressures for etching the various materials [14].

2.3.5 Selectivity

For the selectivity to the underlying material, the ion energy and atom-to-atom bond strength should be considered [15]. Because the reactions proceed in a direction that results in a larger bond strength, it is possible to reduce the etch rate of the underlying material through the selection of gas chemistry based on the bond strength. The selectivity can then be improved. For example, gases based on Br and Cl, whose bond strength with Si is smaller than that of Si–O, might be used for the etching of poly–Si in order to increase the selectivity to the underlying SiO₂. Then the etch rate of the SiO₂ would be extremely low, and a high selectivity would be achieved [16]. This is described in detail in the section on poly–Si etching in the next chapter. Furthermore, another effective approach might be to lower the ion energy in a gas system in which the etch rate dependence on the ion energy is strong for SiO₂ and weak for poly–Si. An F-based gas is the case in point.

Table 2.4 Temperature at which the various chemical compounds achieve a vapor pressure of 1,333 Pa [13]

Chemical compound	Temperature (°C)	Chemical compound	Temperature (°C)	Chemical compound	Temperature (°C)	Chemical compound	Temperature (°C)
AgCl	1,074	CdI ₂	512	HgI ₂	204.5	SbCl ₃	85.2
AgI	983	CrO ₂ Cl ₂	13.8	KBr	982	SbI ₃	223.5
AlBr ₃	118.0	Cu ₂ Br ₂	718	KCl	968	SiCl ₄	-34.7
AlCl ₃	123.8	Cu ₂ Cl ₂	702	KF	1,039	SiClF ₃	-127.0
AlF ₃	1,324	Cu ₂ I ₂	656	KI	887	SiCl ₂ F ₂	-102.9
AlI ₃	225.8	FeCl ₂	700	LiBr	888	SiCl ₃ F	-68.3
As	437	FeCl ₃	235.5	MgCl ₂	930	SiF ₄	-130.4
AsH ₃	-124.7	GeBr ₄	56.8	NaBr	952	SnBr ₄	72.7
BBr ₃	-10.1	GeCl ₄	-15.0	NaF	1,240	SnCl ₂	391
BCl ₃	-66.9	H ₂ S	-116.40	NaI	903	SnCl ₄	10.0
BF ₃	-141.3	H ₂ S ₂	-19	NiCl ₂	759	SnH ₄	-118.5
CdCl ₂	656	H ₂ Se	-100	PbI ₂	571	SnI ₄	175.8
CdF ₂	1,559	HgBr ₂	179.8	PbF ₂	904	ZnCl ₂	508
		HgCl ₂	180.2	SbBr ₃	142.7	ZnF ₂	1,359

2.3.6 Summary

As thus explained, when designing a dry etching process, the etching gas selection and reaction control should be chosen by considering the ion energy dependence of the chemical sputtering yield, the vapor pressures of the etch byproducts, and the atom-to-atom bond strength. In reality, however, it is difficult to satisfy the requirements associated with anisotropy, etch rate, and selectivity all at the same time with a single gas. For example, as Fig. 2.16 shows, Cl-based gases are suited for anisotropic etching of poly-Si. However, Fig. 2.19 shows that a high etch rate is difficult to achieve, because the vapor pressure of the etch byproduct SiCl_4 is lower than that of SiF_4 . The opposite is true with the F-based gases. When designing an actual process, an appropriate mixture of these gases might be used, and a gas that would easily result in the formation of polymers might be mixed in for a sidewall protection process.

References

1. T. Iijima, S. Kondo, T. Aoyama: Plasma Technology, Beginner's Books Series 7, Kogyo Chosakai Publishing Co., Ltd. (1999).
2. Y. Hatta: Gas Discharge, 2nd Edition, Kindai Kagaku Sha Co., Ltd. (1971).
3. M. Tsuda: Plasma Process Technology for Semiconductor, Sangyo Tosho Publishing Co., Ltd., p.23 (1980).
4. H. R. Koenig and L. I. Maissel: IBM J. Res. & Dev. 14, p.168 (1970).
5. B. Chapman: Glow Discharge Processes, John Wiley & Sons (1980).
6. K. Nojiri and E. Iguchi: J. Vac. Sci. & Technol. B 13, 1451(1995).
7. H. Horiike: Proc. 19th Semiconductor Technology Seminar, p.193 (1981).
8. J. W. Coburn and H. F. Winters: J. Appl. Phys. 50, 3189 (1979).
9. S. Tachi: Proc. Symp. Dry Process, p.8 (1983).
10. S. Tachi and S. Okudaira: J. Vac. Sci. Technol. B 4, 459 (1986).
11. K. Nojiri, M. Sadaoka, H. Azuma, K. Kawamura: Ext. Abstr. 36th Spring Meeting of The Japan Society of Applied Physics, No. 2, p.571 (1989).
12. Rikagaku Jiten (Physics and Chemistry Dictionary) 3rd Edition, Iwanami Shoten (1981).
13. Y. Kawamoto: Data Book on Submicron Lithography, Science Forum, p.335 (1985).
14. Kagaku Binran (Handbook of Chemistry): Maruzen Publishing Co., Ltd.
15. Handbook of Chemistry and Physics 47th Edition: The Chemical Rubber Co. (1966).
16. M. Nakamura, K. Iizuka and H. Yano: Jpn. J. Appl. Phys. 28, 2142 (1989).

Dry Etching Technology for Semiconductors

Nojiri, K.

2015, XIII, 116 p. 123 illus., Hardcover

ISBN: 978-3-319-10294-8